ANOMALOUS X-RAY DIFFRACTION FROM ω PARTICLES IN Ti-15Mo ALLOY

Jana ŠMILAUEROVÁ, Petr HARCUBA, Miloš JANEČEK, Václav HOLÝ

Faculty of Mathematics and Physics, Charles University, Prague, EU
smilauerova@karlov.mff.cuni.cz

Abstract

Anomalous X-ray diffraction measurements were performed on a metastable β titanium alloy (Ti-15 wt% Mo) containing thermodynamically metastable ω phase particles. The dependence of diffracted intensity on primary beam energy was measured for selected ω and β diffraction maxima for energies near the MoK absorption edge (20.0 keV). The main focus of the paper is the interpretation of diffuse scattering around the measured β peak. A simulation which qualitatively interprets the observed phenomenon is presented. The proposed model shows that elastic deformation of the β matrix results from both the difference in specific volumes of ω and β phases and a "cloud" of higher Mo content around each ω particle.

Keywords: Metastable β titanium alloys, phase transformations, ω phase, anomalous X-ray diffraction

1. INTRODUCTION

Titanium alloys are a versatile group of materials which can be employed in a number of branches of industry and technology. Due to their outstanding physical properties, such as high specific strength, good corrosion resistance and biocompatibility, metastable β titanium alloys are widely used especially in aerospace and chemical industry, deep-sea drilling, architecture, sport and medicine [1]. Pure titanium is an allotropic material which undergoes a phase transformation at 882 °C from the low-temperature α phase (hexagonal close-packed structure) to the high-temperature β phase (body-centred cubic). Additions of alloying elements can alter the transition temperature (so-called β-transus) and change the stability ranges of each phase. In the following, we will be interested in β-stabilizing elements (e.g. Mo, Fe, V, Nb), which lower the β-transus temperature, effectively widening the stability range of the high-temperature β phase. When the β-stabilizer concentration is high enough, the β phase can be retained upon quenching to room temperature in a metastable state [2]. Such alloys are called metastable β titanium alloys and they provide diverse mechanical properties which can be tailored to a specific application by thermo-mechanical treatment [3-5].

Moreover, new phases can form in the metastable β titanium matrix when certain types and amounts of alloying elements are added. One of the most studied and still not fully understood metastable phases forming in metastable β titanium alloys is the ω phase. ω phase is observed as a very fine distribution of ellipsoidal or cuboidal particles whose size typically ranges from a few nm to a few tens of nm [6,7]. These particles have a hexagonal structure and are coherent with the parent β matrix [6]. It was also reported that ω particles are in the β matrix spatially weakly ordered in a cubic lattice with axes along $\langle 100 \rangle_\beta$ directions [8]. ω phase forms during quenching of the alloy by a diffusionless displacive mechanism which can be described as alternating between collapse of two neighbouring $(111)_\beta$ planes into their intermediate position and leaving the next $(111)_\beta$ plane unchanged [9]. This mechanism produces the hexagonal structure of the ω phase from the bcc β matrix [10]. This transformation is reversible and cannot be suppressed even by extremely fast quenching rates [11]. Due to the nature of this transformation, a specific orientation relationship exists between the β and ω phases [12], namely $(0001)_\omega \parallel (111)_\beta$ and $[11\text{-}20]_\omega \parallel [011]_\beta$. Due to the fact that there are four variants of cubic $(111)_\beta$ planes, there are also four "families" of omega phase particles having a different crystallographic and morphological orientations with respect to the parent β phase. During ageing at low temperatures, typically in

the range of 200 °C - 450 °C, ω particles further evolve by a diffusion-assisted, displacement-controlled process [13,14]. This transformation is accompanied by rejection of alloying elements from the ω phase to the β matrix [15]. It was found that a shell of higher solute content forms around ω particles [16]. However, the evolution of chemical composition of ω particles during ageing is still the subject of discussion. The first estimation of ω phase composition was done by Hickman using transmission electron microscopy [17,18]. The chemical composition of ω particles was studied in aged specimens of Ti-10V2Fe-3Al alloy by the means of a one-dimensional atom probe [19]. More recent research involving three-dimensional atom probe tomography investigated chemical composition of ω phase particles in Ti-Mo [15, 16], Ti-5Al-5Mo-5V-5Cr [20] and Ti-5Al-5Mo-5V2Cr-1Fe alloys [21].

2. MATERIAL AND EXPERIMENTAL METHODS

In this study, the evolution of ω phase particles during ageing in Ti-15 wt.% Mo (Ti-8 at.% Mo) was investigated using anomalous X-ray diffraction (AXRD). This technique makes use of anomalous dependence of diffracted intensity on photon energy in the vicinity of an absorption edge of an element present in the investigated sample. Near the absorption edge, the atomic scattering factor f_0 is modified by a complex dispersion correction

$$f = f_0(\vec{q}) + f'(E) + if''(E), \tag{1}$$

where f' and f'' are the real and imaginary parts of the anomalous dispersion correction, respectively.

For this investigation, single crystals of Ti-15Mo alloy were grown in an optical floating zone furnace. Details of the technique of single crystal growth of metastable β titanium alloys can be found in [22]. Single crystal ingots were solution treated at 860 °C for 4 h in an evacuated quartz tube and subsequently quenched in water. The orientation of the single crystal was determined using Laue back-reflection method (Photonic Science Laue X-ray System) and the OrientExpress software [23]. Disc-shaped samples were cut from the Ti-15Mo single crystal and aged in salt baths, which prevented contamination of the alloy by oxygen. The ageing treatment was terminated by water quenching. The samples were polished using standard metallographic procedures employing SiC papers; a vibratory polisher was used in the final polishing step.

The AXRD experiment was carried out at a dedicated anomalous diffraction and scattering beamline BM02, ESRF, Grenoble, France. The measured energies were in the range of 19.6 keV - 20.6 keV, i.e. in the vicinity of the MoK absorption edge (at 20.0 keV). The sample was mounted on a kappa geometry (four-circle) diffractometer. In order to minimize scattering of the X-ray beam by air, both the incident and diffracted beam path led through evacuated tubes. The diffracted intensity was detected by a 2D detector IMXPAD S70.

3. RESULTS AND DISCUSSION

In this experiment, the dependence of diffracted intensity on the primary beam energy was measured for selected β and ω diffraction maxima. In particular, $(44\text{-}82)_\omega$ and $(006)_\beta$ maxima were investigated. Examples of detector images showing these diffraction peaks are shown in **Figure 1** (the two vertical lines with no intensity arise from masking the region of partial overlap of detector chips). In this as well as in the following figures, we used the reciprocal-space coordinates q_x and q_y of the reciprocal-space vector defined with respect to the reciprocal-lattice point $q = K_f - Ki - h \equiv Q - h$, where $K_{i,f}$ are the wave vectors of the primary and scattered waves, Q is the scattering vector, and h is the reciprocal-lattice vector. The $q_{x,y}$ coordinates lie in the detector plane perpendicular to K_f.

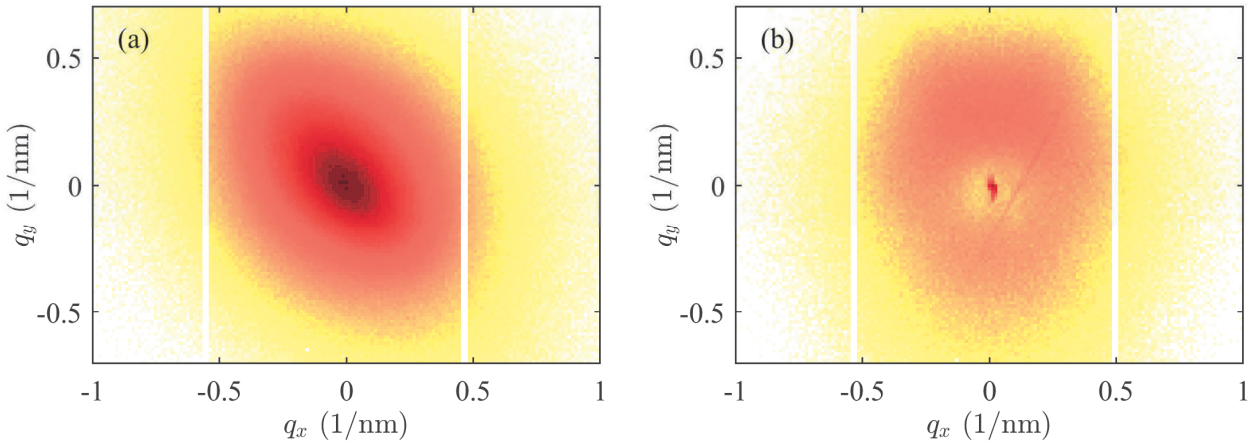

Figure 1 Examples of (a) $(44\text{-}82)_\omega$ and (b) $(006)_\beta$ diffraction peaks for single crystal of Ti-15Mo aged at 370°C for 64 h

The $(44\text{-}82)_\omega$ maximum, see **Figure 1(a)**, exhibits an ellipsoidal shape which is caused by the ellipsoidal shape of ω particles. It was previously shown that these diffuse maxima arising from the ω phase can be directly related to the size and shape of ω particles in the material [24]. The following discussion will focus on the evolution of the β diffraction peak and the diffuse scattering in its vicinity. The $(006)_\beta$ diffraction peak contains sharp and broad components, see **Figure 1(b)**. The sharp "coherent" maximum (near the origin of the reciprocal space) stems from the undisturbed part of the sample volume, and its width is entirely determined by the resolution of the experimental setup. The broad component is caused by diffuse scattering from the contrast of the structure factors of the ω particles and the β matrix (chemical contrast), as well as from the elastic displacement field around the particles, and possibly from other structural defects present in the sample. In the following, we will analyse the diffuse scattering around the $(006)_\beta$ diffraction peak in detail. In order to discriminate the influence of the chemical contrast from the elastic strain, we measured the energy dependence of diffuse scattering around the MoK absorption edge. In **Figure 2** we plotted the energy dependence of diffuse scattering obtained from various rectangular ranges of interest (ROIs) depicted as black squares in **Figure 2(a)**. **Figure 2(b)** demonstrates that the energy profiles of various ROIs substantially differ. In particular, the ROIs 1-4 situated at negative q_y exhibit a sharp maximum at the energy just below the absorption edge, while the other ROIs (5-8) show round profiles in this energy range.

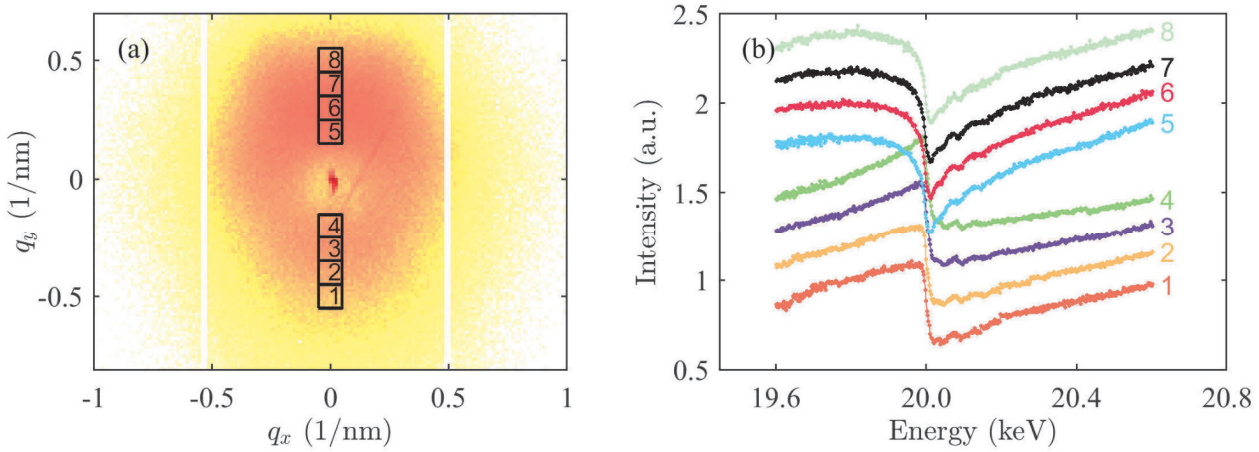

Figure 2 Dependence of intensity on primary beam energy for different ROIs

In this paper we present only a qualitative explanation of this interesting phenomenon, a detailed comparison of the measured and simulated data will be subject of a future publication. We show that this effect is a proof

of presence of (i) a "cloud" of enhanced Mo concentration around each ω particle, and (ii) an elastic strain field resulting from a difference in specific volumes of ω and β phases.

The simulation of diffuse scattering is based on standard theory of diffuse scattering yielding the following "master formula" for diffusely scattered intensity [25, 26]

$$I_{\vec{h}}(\vec{q}) = nA\left|\Psi_{\vec{h}}(\vec{q})\right|^2,\ \ \Psi_{\vec{h}}(\vec{q}) = \int d^3\vec{r}\, e^{-i\vec{q}\cdot\vec{r}}\left[\chi_{\vec{h}}(\vec{r},E)\, e^{-i\vec{h}\cdot\vec{u}(\vec{r})} - \chi_{\vec{h}}^{\mathrm{matrix}}(E)\right], \tag{2}$$

where *n* is the number density of ω particles, *A* is a constant containing, among others, the intensity of the primary wave and the polarization factor, $\vec{u}(\vec{r})$ is the displacement field around an ω particle, $\chi_{\vec{h}}(\vec{r},E)$ is the polarizability of an ω particle and the Mo cloud around it, and $\chi_{\vec{h}}^{\mathrm{matrix}}(E)$ is the polarizability of the β matrix. The polarizabilities depend on the energy *E*. The former is proportional to the weighted average of the Ti and Mo atomic form factors (and hence it depends on the local Mo concertation $c_{\mathrm{Mo}}(\vec{r})$ in a Mo-rich cloud around a particle), while the latter is assumed position-independent and it contains the average Mo content *c* in the β matrix. The values of atomic form-factors were taken from [27].

We calculated the displacement field $\vec{u}(\vec{r})$ around an ω particle using the approach of elastic Green function [24] assuming that the particles are elongated in the respective $[111]_\beta \equiv [0001]_\omega$ crystallographic directions, and that they deform the surrounding lattice; the density of volume force acting on the surrounding matrix depends on the lattice ω/β misfits $f_{\perp,\parallel}$ across and along the $[0001]_\omega$ particle axis. A Mo-rich cloud represents another source of deformation; we assumed that the Mo concentration depends exponentially on the distance from the particle centre: $c_{\mathrm{Mo}}(r) = (c_0 - c_{\mathrm{matrix}})\exp\left(-\frac{r}{\xi}\right) + c_{\mathrm{matrix}}$. The value of Mo/Ti mismatch from [28] was used.

In the following figures we present typical simulation results and draw qualitative conclusions from comparison with experimental data. In all figures we assumed $c_{\mathrm{matrix}} = 0.08$, which corresponds to the nominal Mo concentration (it at.%) in investigated samples. **Figure 3** presents the simulated detector image and the energy dependences of chosen ROI signals calculated for spherical ω particles with radius *R* = 6 nm without any Mo cloud and with no elastic deformation around them. From the figure it is obvious that the energy dependent ROI signals are almost identical and the experimental finding in **Figure 2** (i.e. differing energy dependences of integrated intensities in different ROIs) cannot be reproduced.

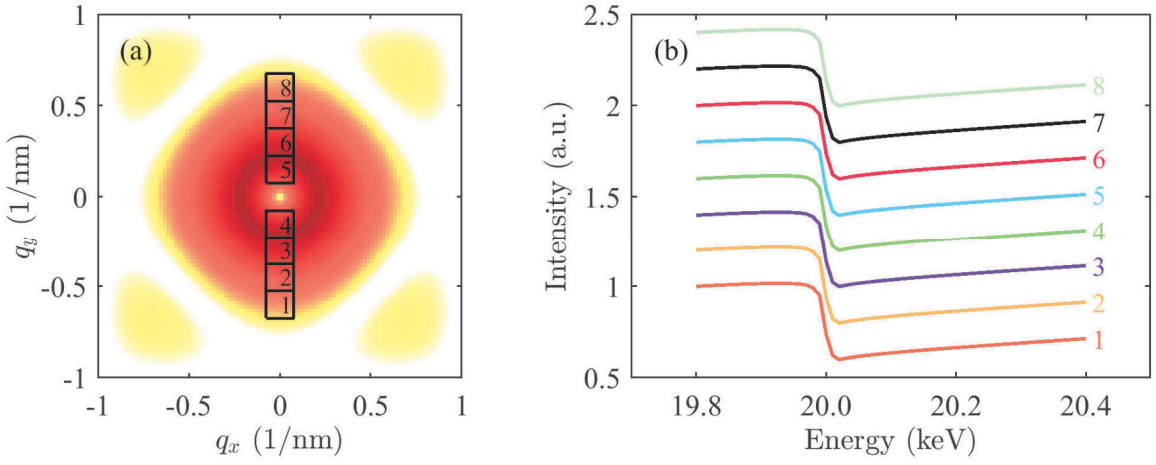

Figure 3 (a) Simulated detector image and (b) energy dependences of ROI signals calculated for spherical particles without a Mo cloud and without elastic deformation (the curves are shifted vertically for clarity)

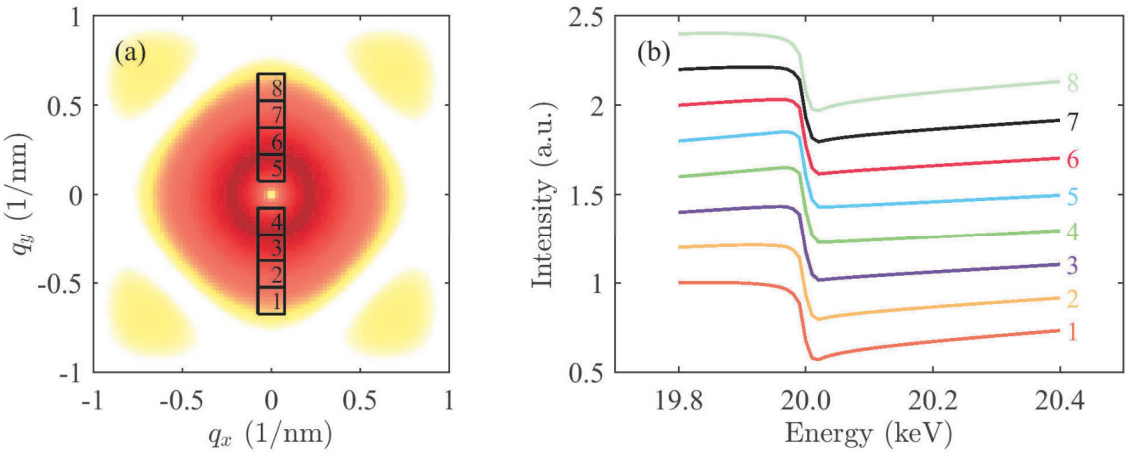

Figure 4 (a) Simulated detector image and (b) energy dependences of ROI signals calculated for spherical particles with Mo cloud, no elastic deformation is taken into account

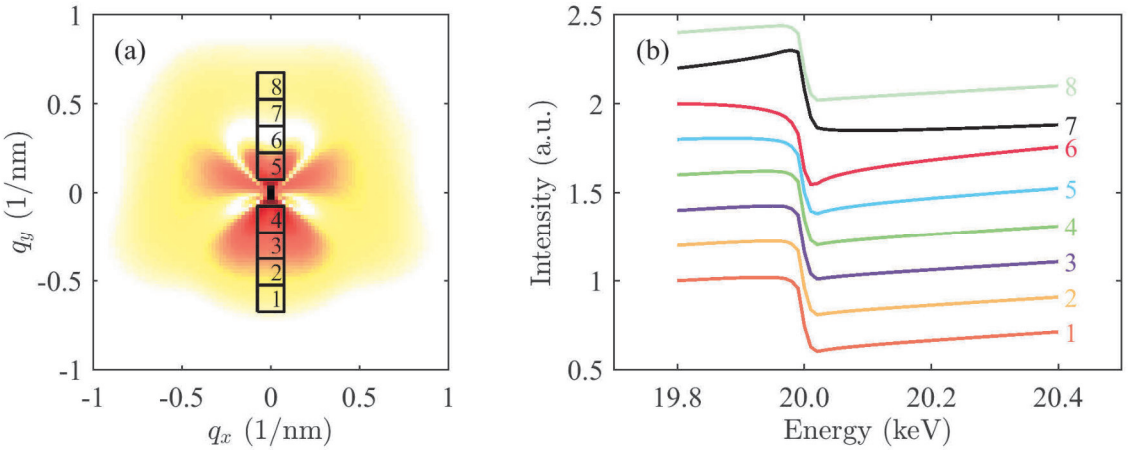

Figure 5 (a) Simulated detector image and (b) energy dependences of ROI signals calculated for ellipsoidal particles, elastic deformation from the Mo cloud is included

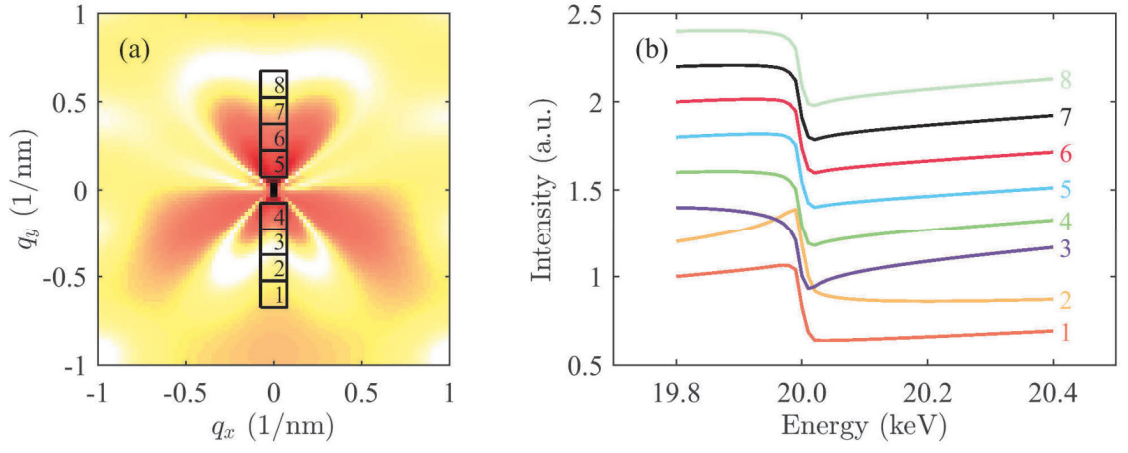

Figure 6 (a) Simulated detector image and (b) energy dependences of ROI signals calculated for ellipsoidal particles, elastic deformation from the Mo cloud as well as from ω particles is included

In **Figure 4**, the simulation results assuming spherical particles of the same size, however accompanied with a Mo cloud with the parameters $c_0 = 0.2, \xi = 1$ are presented. The detector image is almost identical with that in **Figure 3**, the ROI signals are slightly different, but they are not consistent (at least qualitatively) with the experimental data. A slight improvement was achieved by considering an ellipsoidal shape of ω particles (half-axes of the prolate ellipsoid being 4 and 6 nm) and the elastic strains originating from the Mo cloud, see **Figure 5**. **Figure 6** was obtained by including the elastic strains from the Mo cloud and from the ω particle itself into the simulation; for the calculation of the latter we used the mismatch values of $f_{\parallel} = f_{\perp} = 0.01$.

4. CONCLUSION

In this study, the simulations of anomalous X-ray diffraction measurements performed on Ti-15Mo alloy in the vicinity of the MoK absorption edge (20.0 keV) were presented. In particular, the main focus was on diffuse scattering around the $(006)_{\beta}$ diffraction maximum. It was shown that the best qualitative agreement with experimental data is achieved when (i) ellipsoidal ω particles are considered, (ii) a "cloud" of higher Mo concentration is present around ω particles and this cloud elastically deforms the β matrix, and (iii) elastic deformation of the β matrix due to ω lattice mismatch is included. It should be noted that a complete agreement with experimental data has not yet been reached; however, the model is in principle able to capture qualitatively the behaviour of diffuse scattering around the β diffraction peak.

ACKNOWLEDGEMENTS

This work was financially supported by the Czech Science Foundation, project no. 16-12598S.

REFERENCES

[1] LUTJERING, G. and WILLIAMS, J. C. *Titanium*. 2nd ed. Berlin: Springer, 2007.

[2] LEYENS, C. and PETERS, M. *Titanium and titanium alloys*. Weinheim: Wiley-VCH, 2003.

[3] BANERJEE, D. and WILLIAMS, J. C. Perspectives on titanium science and technology. *Acta Materialia*. 2013. vol. 61, pp. 844-879.

[4] FANNING, J. C. and FOX. S. P. Recent developments in metastable β strip alloys. *Journal of Materials Engineering and Performance*. 2005. vol. 14, no. 6, pp. 703-708.

[5] LAHEURTE, P., PRIMA, F., EBERHARDT, A., GLORIANT, T., WARY, M. and PATOOR, E. Mechanical properties of low modulus β titanium alloys designed from the electronic approach. *Journal of the Mechanical Behavior of Biomedical Materials*. 2010. vol. 3, pp. 565-573.

[6] WILLIAMS, J. C. Critical review: Kinetics and phase transformations. *Titanium Science and Technology*. 1973. vol. 3, pp. 1433-1494.

[7] WILLIAMS, J. C. and BLACKBURN, M. J. The influence of misfit on the morphology and stability of the omega phase in titanium-transition metal alloys. *Transactions of the Metallurgical Society of AIME*. 1969. vol. 245, pp. 2352-2355.

[8] ŠMILAUEROVÁ, J., HARCUBA, P., STRÁSKÝ, J., STRÁSKÁ, J., JANEČEK, M., POSPÍŠIL, J., KUŽEL, R., BRUNÁTOVÁ, T., HOLÝ, V. and ILAVSKÝ, J. Ordered array of ω particles in β-Ti matrix studied by small-angle X-ray scattering. *Acta Materialia*. 2014. vol. 81, pp. 71-82.

[9] DE FONTAINE, D. Mechanical instabilities in the b.c.c. lattice and the beta to omega phase transformation. *Acta Metallurgica.* 1970. vol. 18, pp. 275-279.

[10] DE FONTAINE, D. Simple models for the omega transformation. *Metallurgical Transactions A*. 1988. vol. 19, pp. 169-175.

[11] BAGARJATSKIJ, J. A., NOSOVA, G. I. and TAGUNOVA, T. V. On the nature of the omega phase in quenched titanium alloys. *Acta Crystallographica*. 1961. vol. 14, pp. 1087-1088.

[12] SILCOCK, J. M. An X-ray examination of the ω phase in TiV, TiMo and TiCr alloys. *Acta Metallurgica*. 1958. vol. 6, no. 7, pp. 481-493.

[13] HICKMAN, B. S. The formation of omega phase in titanium and zirconium alloys: A review. *Journal of Materials Science*. 1969. vol. 4, pp. 554-563.

[14] DUERIG, T. W., TERLINDE, G. T. and WILLIAMS, J. C. The ω-phase reaction in titanium alloys. In Titanium '80 Science & Technology Proceedings of the 4th Int. Conference on Titanium. Warrendale, PA: KIMURA, H. and IZUMI, O., eds., 1980, pp. 1299-1308.

[15] DEVARAJ, A., NAG, S., SRINIVASAN, R., WILLIAMS, R. E. A., BANERJEE, S., BANERJEE, R. and FRASER, H. L. Experimental evidence of concurrent compositional and structural instabilities leading to ω precipitation in titanium-molybdenum alloys. *Acta Mateialia*. 2012. vol. 60, pp. 596-609.

[16] DEVARAJ, A., WILLIAMS, R. E. A., NAG, S., SRINIVASAN, R., FRASER, H. L. and BANERJEE, R. Three-dimensional morphology and composition of omega precipitates in a binary titanium-molybdenum alloy. *Scripta Materialia*. 2009. vol. 61, pp. 701-704.

[17] HICKMAN, B. S. Omega phase precipitation in alloys of titanium with transition metals. *Transactions of the Metallurgical Society of AIME*. 1969. vol. 245, pp. 1329-1336.

[18] HICKMAN, B. S. Precipitation of the omega phase in titanium-vanadium alloys. *Journal of the Institute of Metals*. 1968. vol. 96, pp. 330-337.

[19] HADJADJ, L., CAMPAGNAC, M. H., VASSEL, A. and MENAND, A. Atom-probe and TEM study of the isothermal ω and secondary α phases in a Ti-10V-2Fe-3Al alloy. *Microscopy Microanalysis Microstructures*. 1992. vol. 3, pp. 471-482.

[20] COAKLEY, J., VORONTSOV, V. A., JONES, N. G., RADECKA, A., BAGOT, P. A. J., LITTRELL, K. C., HEENAN, R. K., HU, F., MAGYAR, A. P., BELL, D. C. and DYE, D. Precipitation processes in the beta-titanium alloy Ti-5Al-5Mo-5V-3Cr. *Journal of Alloys and Compounds*. 2015. vol. 646, pp. 946-953.

[21] AHMED, M., LI, T., CASILLAS, G., CAIRNEY, J. M., WEXLER, D. and PERELOMA, E. V. The evolution of microstructure and mechanical properties of Ti-5Al-5Mo-5V-2Cr-1Fe during ageing. *Journal of Alloys and Compounds*. 2015. vol. 629, p. 260-273.

[22] ŠMILAUEROVÁ, J., POSPÍŠIL, J., HARCUBA, P., HOLÝ, V. and JANEČEK, M. Single crystal growth of TIMETAL LCB titanium alloy by a floating zone method. *Journal of Crystal Growth*. 2014. vol. 405, pp. 92-96.

[23] LAUGIER, J. and BOCHU, B. OrientExpress Version 3.4. École Nationale Supérieure de Physique de Grenoble. 2005. [Online]. Available: http://www.ccp14.ac.uk/tutorial/lmgp/orientexpress.htm.

[24] ŠMILAUEROVÁ, J., HARCUBA, P., POSPÍŠIL, J., MATĚJ, Z. and HOLÝ V. Growth of ω inclusions in Ti alloys: An X-ray diffraction study. *Acta Materialia*. 2013. vol. 61, no. 17, pp. 6635 - 6645.

[25] KRIVOGLAZ, M. A. *X-Ray and Neutron Diffraction in Nonideal Crystals*. Berlin Heidelberg: Springer, 1996.

[26] PIETSCH, U., HOLÝ, V. and BAUMBACH, T. *High-Resolution X-Ray Scattering; From Thin Films to Lateral Nanostructures*. New York: Springer, 2004.

[27] "Henke Tables," [Online]. Available: http://henke.lbl.gov/optical_constants/.

[28] CAO, P., TIAN, F. and WANG, Y. Effect of Mo on the phase stability and elastic mechanical properties of Ti-Mo random alloys from ab initio calculations. *Journal of Physics: Condensed Matter*. 2017. vol. 29, p. 435703.